ОБЪЕДИНЕННЫЙ
ИНСТИТУТ
ЯДЕРНЫХ
ИССЛЕДОВАНИЙ

Дубна

E2-2003-51

A. E. Dorokhov[1], A. E. Radzhabov[2], M. K. Volkov[3]

$SU(2) \times SU(2)$ CHIRAL QUARK MODEL WITH NONLOCAL INTERACTION

Submitted to «Ядерная физика»

[1]E-mail address: dorokhov@thsun1.jinr.ru
[2]E-mail adress: aradzh@thsun1.jinr.ru
[3]E-mail address: volkov@thsun1.jinr.ru

2003

1. INTRODUCTION

Chiral symmetry is one of the basic symmetries of hadron interactions [1]. The phenomenological Lagrangians successfully describing interactions of light baryons and mesons were constructed forty years ago[2]. That time the Nambu–Jona-Lasinio (NJL) model was proposed where the authors attempted to explain the origin of the nucleon mass by spontaneous breaking of chiral symmetry [3].

In 1976, this model was used for construction of the chiral-symmetric four-quark interaction that after bosonization leads to the phenomenological meson Lagrangians obtained earlier [4]. This model was developed in [5, 6] and after that was widely utilized by many authors [7]. The quark NJL model can be successfully used to obtain not only the phenomenological Lagrangians but also the mass spectrum of mesons, the relations between the strong coupling constants in the scalar-pseudoscalar and vector–axial-vector sectors. In this model it is also possible to describe the breaking of the $SU(3)$ symmetry taking into account the mass difference of strange and u , d quarks. This explains the inequality of the weak decay constants f_π and f_K, and the differences of the strange and non-strange meson masses. Including the gluon anomalies in the consideration allows us to solve the $U_A(1)$ problem and to describe the mass difference of the η, η' mesons [6].

However, the NJL models has some defects. They contain ultraviolet (UV) divergences and do not provide quark confinement. Usually, UV divergences are removed by using the cut-off parameter Λ taken at energy scale of the order of 1 GeV. The physical meaning of this cut-off is connected with the separation of the energy-momentum region where spontaneous breaking of the chiral symmetry and bosonization of quarks take place. Unfortunately, this procedure is not unique and can be realized in different ways. However, it is worth noting that, as a rule, the different schemes of UV cut-off lead to close results.

Right after the discovery of the nontrivial classical solutions in QCD, instantons [8], it was recognized that they might be important in hadron physics. Indeed, it was shown, in particular, that the instanton induced nonlocal quark - quark interaction provides a mechanism explaining the spontaneous breaking of chiral symmetry [10] and the $U_A(1)$ problem [9]. Later on, within the realistic instanton liquid model of QCD vacuum [11] the main features of the spectrum of light mesons and baryons have been described [12].

The instanton induced quark-quark interaction being nonlocal naturally regularizes the UV divergencies in an analytical form. So, in the instanton model the UV cut-off results from the internal nonlocal structure of the nonperturbative QCD vacuum. At the same time, the model does not explain the quark confinement. This problem becomes essential in the description of hadrons with masses exceeding the sum of constituent quark masses.

There are many works devoted to the construction of nonlocal quark models providing quark confinement[13–20]. In these models the dynamical quark mass depends on momentum. One of the models of this kind is considered here. The nonlocal four-quark interaction is taken in a separable form motivated by the instanton model. However, a more general space-spin-flavor structure of the quark interaction is allowed than it is followed from the quark zero mode arguments. Namely, the four-fermion couplings in different channels are fixed directly from the meson mass spectrum. Further, we use one of the simplest ansätze for the nonlocal kernel which allows us to obtain the dynamically generated quark propagator without poles. Our model is close to the model [17]. However, our choice of the nonlocal kernel is motivated by the existence of the nonlocal quark condensate in QCD.

The paper is organized as follows. In Sect.2, we consider a nonlocal four-quark interaction and after bosonization derive the gap equation for dynamical quark mass. The nonlocal kernel is defined in Sect.3. In Sect.4, the masses and couplings of the scalar and pseudoscalar mesons are obtained and the main parameters of the model are fixed. The verification of the Goldberger-Treiman relation is given. In Sect.5, calculations of the ρ-meson coupling constant, g_ρ, and the decay width $\rho \to \pi\pi$ are given . The axial-vector meson, a_1, and the $\pi - a_1$ mixing are also considered. The last section is devoted to the discussion of our results.

2. $SU(2) \times SU(2)$ QUARK MODEL WITH NONLOCAL INTERACTION

The $SU(2) \times SU(2)$ symmetric action with the nonlocal four-quark interaction has the form

$$\mathcal{S}(\bar{q},q) = \int d^4x \left\{ \bar{q}(x)(i\hat{\partial}_x - m_c)q(x) + \frac{G_\pi}{2}\left(J_\sigma(x)J_\sigma(x) + J^a_\pi(x)J^a_\pi(x)\right) \right.$$
$$\left. -\frac{G_\rho}{2} J^{\mu\,a}_\rho(x)J^{\mu\,a}_\rho(x) - \frac{G_{a_1}}{2} J^{\mu\,a}_{a_1}(x)J^{\mu\,a}_{a_1}(x) \right\}, \qquad (1)$$

where $\bar{q}(x) = (\bar{u}(x), \bar{d}(x))$ are the u and d quark fields, m_c is the diagonal matrix of the current quark masses. The nonlocal quark currents $J_I(x)$ are expressed as

$$J_I(x) = \int\int d^4x_1 d^4x_2\, f(x_1) f(x_2)\, \bar{q}(x-x_1)\,\Gamma_I\, q(x+x_2), \tag{2}$$

where the nonlocal function $f(x)$ normalized by $f(0)=1$ characterizes the space dependence of the quark condensate. In (2) the matrices Γ_I are defined as

$$\Gamma_\sigma = 1, \Gamma_\pi^a = i\gamma^5\tau^a, \Gamma_\rho^{\mu\,a} = \gamma^\mu\tau^a, \Gamma_{a_1}^{\mu\,a} = \gamma^5\gamma^\mu\tau^a,$$

where τ^a are the Pauli matrices and γ^μ, γ^5 are the Dirac matrices.

In this article, we mainly consider the strong interactions. The electroweak fields may be introduced by gauging the quark field by the Schwinger phase factors (see, c.f. [17, 21, 22]). This method is used in derivation of the Goldberger-Treiman relation.

After bosonization the action becomes

$$S(q,\bar{q},\sigma,\pi,\rho,a) = \int d^4x \left\{ -\frac{1}{2G_\pi}\left(\tilde{\sigma}(x)^2 + \pi^a(x)^2\right) + \frac{1}{2G_\rho}(\rho^{\mu\,a}(x))^2 + \frac{1}{2G_{a_1}}(a_1^{\mu\,a}(x))^2 + \right.$$
$$\bar{q}(x)(i\hat{\partial}_x - m_c)q(x) + \int\int d^4x_1 d^4x_2\, f(x-x_1) f(x_2-x)\, \bar{q}(x_1)\left(\tilde{\sigma}(x) + \pi^a(x) i\gamma^5\tau^a + \right.$$
$$\left.\left. +\rho^{\mu\,a}(x)\gamma^\mu\tau^a + a_1^{\mu\,a}(x)\gamma^5\gamma^\mu\tau^a\right) q(x_2)\right\}, \tag{3}$$

where $\tilde{\sigma}, \pi, \rho, a$ are the σ, π, ρ, a_1 meson fields, respectively. The field $\tilde{\sigma}$ has a nonzero vacuum expectation value $<\tilde{\sigma}>_0 = \sigma_0 \neq 0$. In order to obtain a physical scalar field with zero vacuum expectation value it is necessary to shift the scalar field as $\tilde{\sigma} = \sigma + \sigma_0$. This leads to appearance of the nonlocal quark mass $m(p)$ instead of the current quark mass m_c

$$m(p) = m_c + m_{dyn}(p) = m_c - \sigma_0 f^2(p) = m_c + (m_q - m_c) f^2(p), \tag{4}$$

where m_q is dimensional parameter which play the role of the constituent quark mass. These relations result from the solution of the gap equation

$$m(p) = m_c + iG_\pi \frac{2N_c}{(2\pi)^4} f^2(p) \int d^4k\, f(k)^2 \mathrm{Tr}\left[S(k)\right] \tag{5}$$

that one derived from the action, Eq. (3), by using

$$\left\langle \frac{\delta S}{\delta\sigma} \right\rangle_0 = 0. \tag{6}$$

In the leading order of the $1/N_c$ expansion the inverse quark propagator with dynamical mass is given by

$$S^{-1}(p) = \hat{p} - m(p). \tag{7}$$

3. DYNAMICAL QUARK MASS

Let us remind that in the instanton model the nonlocal function $f(p)$ defining the kernel of the nonlocal four - quark interaction is expressed in terms of the profile function of the quark zero mode. In [17], taking the same separable form of the kernel the function $f(p)$ was chosen in the Gaussian form. This choice also removes UV divergencies but in addition provides the quark confinement. Here, we follow different ideology. Namely, close to [13] we demand absence of pole singularities in the scalar part of the quark propagator

$$\frac{m(p^2)}{m^2(p)+p^2} \equiv \frac{1}{2}Q(p^2). \tag{8}$$

This equation is given in the Euclidean domain of p^2. Note, that the left side of (8) coincides with the nonlocal quark condensate if the quark propagator is taken in the form (7) [23]. The function $Q(p^2)$ is considered as an entire function in the complex p^2 plane decreasing in the Euclidean domain at $p^2 \to \infty$. In particular, in this work the Gaussian function is used

$$Q(p^2) = \frac{1}{\mu}\exp\left(-\frac{p^2}{\Lambda^2}\right), \tag{9}$$

where μ and Λ are arbitrary parameters. At each p eq. (8) has the following solutions

$$m_\pm(p) = Q^{-1}(p^2)\left(1 \pm \sqrt{1-p^2Q^2(p^2)}\right). \tag{10}$$

Then three different situations occur:

1. There is some region of real p^2 where $p^2Q^2(p^2) > 1$. This situation leads to the appearance of complex values of the quark mass. We do not consider this case further.

2. The relation $p^2Q^2(p^2) < 1$ is fulfilled in the whole domain of real p^2. Then from two possible solutions we can use only the solution $m_-(p)$ which decreases at $p^2 \to \infty$

$$m(p) = m_-(p) = Q^{-1}(p^2)\left(1 - \sqrt{1-p^2Q^2(p^2)}\right). \tag{11}$$

3. The function $p^2Q^2(p^2)$ equals 1 at a single real point p_0^2. In this case the continuous mass function is

$$m(p) = Q^{-1}(p^2)\left(1 - \mathrm{sgn}(p^2-p_0^2)\sqrt{1-p^2Q^2(p^2)}\right).$$

The last case is defined by conditions

$$p^2Q^2(p^2)|_{p^2=p_0^2} = 1, \quad (p^2Q^2(p^2))'|_{p^2=p_0^2} = 0, \tag{12}$$

that constrains the model parameters m_q and Λ as

$$p_0^2 = \frac{\Lambda^2}{2}, \quad \mu^2 = \frac{\Lambda^2}{2e}, \quad m_q = 2\mu. \tag{13}$$

As a result only one parameter remains free. This is due to equivalence of the third case to the choice of normalization condition $m(p^2 = p_0^2) = \sqrt{p_0^2}$.

If the current quark mass m_c is nonzero, eqs.(9) and (10) are modified as follows:

$$\begin{aligned} \frac{m_{dyn}(p)}{m^2(p)+p^2} &= \frac{1}{2}Q(p^2), \\ m_{dyn\pm}(p) &= Q^{-1}(p^2) - m_c \pm \sqrt{(Q^{-1}(p^2) - m_c)^2 - (p^2 + m_c^2)}, \end{aligned} \tag{14}$$

and eq.(13) becomes

$$p_0^2 = \frac{\Lambda^2}{2}\epsilon, \quad \epsilon = \left(1 - \frac{m_c^2}{\Lambda^2} - \frac{m_c}{\Lambda}\sqrt{2 + \frac{m_c^2}{\Lambda^2}}\right), \tag{15}$$

$$\mu^2 = \Lambda^2 \exp(-\epsilon)\left(1 - \frac{\epsilon}{2}\right), \quad m_q = \mu\left(1 + \sqrt{1 - 2\frac{m_c}{\mu}}\right). \tag{16}$$

We checked that in the second case the model with Gaussian nonlocality (9) predicts the σ-meson mass and decays $\sigma \to \pi\pi$, $\rho \to \pi\pi$ that are in disagreement with experiment. The third case allows us to construct the scheme where not only the main low-energy theorems are fulfilled, but also the better agreement with experimental data is achieved. Therefore, the present work is devoted to investigation of this case.

4. PSEUDOSCALAR AND SCALAR MESONS.

Let us consider the scalar and pseudoscalar mesons. The meson propagators are given by

$$D_{\sigma,\pi}(p^2) = \frac{1}{-G_\pi^{-1} + \Pi_{\sigma,\pi}(p^2)} = \frac{g_{\sigma,\pi}^2(p^2)}{p^2 - M_{\sigma,\pi}^2}, \tag{17}$$

where $M_{\sigma,\pi}$ are the meson masses, $g_{\sigma,\pi}(p^2)$ are the functions describing renormalization of the meson fields and $\Pi_{\sigma,\pi}(p^2)$ are the polarization operators (see fig. 1) defined by

$$\Pi_{\sigma,\pi}(p^2) = i\frac{2N_c}{(2\pi)^4}\int d^4k f^2(k_-^2) f^2(k_+^2)\, \mathrm{Sp}\left[S(k_-)\Gamma_{\sigma,\pi}S(k_+)\Gamma_{\sigma,\pi}\right], \tag{18}$$

where $k_+ = k + p/2$, $k_- = k - p/2$. The meson masses $M_{\sigma,\pi}$ are found from the position of the pole in the meson propagator

$$\Pi_{\sigma,\pi}(M^2_{\sigma,\pi}) = G_\pi^{-1}, \tag{19}$$

and the constants $g_{\sigma,\pi}(M^2_{\sigma,\pi})$ are given on meson mass shell by (see also fig.2)

$$g^{-2}_{\sigma,\pi}(M^2_{\sigma,\pi}) = \frac{d\Pi_{\sigma,\pi}(p^2)}{dp^2}|_{p^2=M^2_{\sigma,\pi}}. \tag{20}$$

In the chiral limit the pion constant $g_\pi(0)$ is given by [24]

$$g_\pi^{-2}(0) = \frac{N_c}{4\pi^2 m_q^2}\int\limits_0^\infty du\, u \frac{m^2(u) - u\, m(u) m'(u) + u^2 m'^2(u)}{(u+m^2(u))^2}. \tag{21}$$

4.1. *Pion mass*

Describing the pion properties we can consider only the lowest order of the expansion in small p^2. Indeed, in our model $M_\pi^2 \ll m_q^2, \Lambda^2$ (see the end of this section). In this approximation one gets

$$M_\pi^2 = g_\pi^2(0)\left(\frac{1}{G_\pi} - \frac{N_c}{2\pi^2}\int\limits_0^\infty du\, u \frac{f(u)^4}{u+m^2(u)}\right). \tag{22}$$

On the other hand, the constant G_π is defined by the gap equation ($m_q \equiv m(0)$) is

$$\begin{aligned}\frac{1}{G_\pi} &= \frac{1}{m_q - m_c}\frac{N_c}{2\pi^2}\int\limits_0^\infty du\, u \frac{f(u)^2 m(u)}{u+m^2(u)} = \\ &= \frac{N_c}{2\pi^2}\int\limits_0^\infty du\, u \frac{f(u)^4}{u+m^2(u)} + m_c \cdot \frac{1}{m_q^2}\frac{N_c}{2\pi^2}\int\limits_0^\infty du\, u \frac{m_{dyn}(u)}{u+m^2_{dyn}(u)} + O(m_c^2).\end{aligned} \tag{23}$$

As a result, the pion mass equals

$$M_\pi^2 = -2m_c \frac{g_\pi^2(0)}{m_q^2}\left(-\frac{N_c}{4\pi^2}\int\limits_0^\infty du\, u \frac{m_{dyn}(u)}{u+m^2_{dyn}(u)}\right) + O(m_c^2). \tag{24}$$

It is worth noting that the expression in the parentheses represents the quark condensate in the chiral limit $m_c = 0$. Hence, the Gell-Mann–Oakes–Renner relation is reproduced

$$M_\pi^2 \approx -2\frac{g_\pi^2}{m_q^2} m_c \langle\bar{q}q\rangle_0. \tag{25}$$

4.2. Goldberger-Treiman relation

For description of the decay $\pi \to \mu\nu$ the external weak field must be introduced. We use the method consisting of the replacement the quark fields in the interaction part of Lagrangian by the quark fields with Schwinger factors depending on external weak field. This procedure ensures the gauge-invariance of the interaction with respect to the weak field.

The amplitude of the process $\pi \to \mu\nu$ has the form

$$A^{\mu}_{(\pi\to\mu\nu)}(p) = ip^{\mu}F_{\pi}, \tag{26}$$

where F_π is the weak pion decay constant $F_\pi = 93$ MeV [25]. The diagrams of fig.3 give the following contributions:

$$\begin{aligned}
F_\pi^{(1)} &= \frac{N_c}{p^2}g_\pi \int \frac{d^4k}{(2\pi)^4} f(k_+)f(k_-)\mathrm{Tr}[i\gamma^5 S(k_-)\hat{p}\gamma^5 S(k_+)],\\
F_\pi^{(2)} &= i\frac{N_c}{p^2}g_\pi \int \frac{d^4k}{(2\pi)^4}\mathrm{Tr}[S(k)]f(k)(f(k+p)+f(k-p)-2f(k)),\\
F_\pi^{(3)} &= \frac{m_q N_c}{p^2}g_\pi \int \frac{d^4k}{(2\pi)^4} f(k_+)f(k_-)\mathrm{Tr}[i\gamma^5 S(k_-)\gamma^5 S(k_+)](f(k_+)-f(k_-))^2,
\end{aligned} \tag{27}$$

that in the chiral limit at $p^2 = 0$ are reduced to

$$\begin{aligned}
F_\pi^{(1)} &= \frac{g_\pi}{m_q}\cdot\frac{N_c}{8\pi^2}\cdot\int_0^\infty du\, u\frac{m(u)(2m(u)-um'(u))}{(u+m(u)^2)^2},\\
F_\pi^{(2)} + F_\pi^{(3)} &= \frac{g_\pi}{m_q}\cdot\frac{N_c}{8\pi^2}\int_0^\infty du\, u\frac{um'^2(u) - 2m(u)m'(u) - u\, m(u)m''(u)}{u+m(u)^2}.
\end{aligned}$$

Summing all terms and using (21) one obtains the Goldberger-Treiman relation

$$F_\pi = F_\pi^{(1)} + F_\pi^{(2)} + F_\pi^{(3)} = \frac{g_\pi}{m_q}\frac{N_c}{4\pi^2}\int_0^\infty du\, u\frac{m^2(u) - um(u)m'(u) + u^2m'^2(u)}{(u+m(u)^2)^2} = \frac{m_q}{g_\pi}. \tag{28}$$

4.3. Numerical estimations

First, let us consider the chiral limit $m_c = 0$. Three model parameters m_q, Λ, G_π are defined from (5), (13), (28)

$$\Lambda = 406\,\mathrm{MeV},\ G_\pi = 63\,\mathrm{GeV}^{-2},\ m_q = 348\,\mathrm{MeV} \tag{29}$$

(in this case $g_\pi(0) = 3.7$). If $m_c \neq 0$ by using also equation (25) with $M_\pi = 140$ MeV one obtains very close numbers

$$\Lambda = 400\,\mathrm{MeV},\ G_\pi = 61\,\mathrm{GeV}^{-2},\ m_q = 346\,\mathrm{MeV},\ m_c = 14.5\,\mathrm{MeV} \tag{30}$$

(in this case $g_\pi(M_\pi) = 3.6$).

4.4. *Sigma meson*

By using the parameters (30) we get $M_\sigma = 450$ MeV and $g_\sigma(M_\sigma) = 3.8$. The amplitude of the decay $\sigma \to \pi\pi$ described by the diagram in fig.(4) is equal to $A_{(\sigma\to\pi^+\pi^-)} = 1.5$ GeV. Then the total decay width is $\Gamma_{(\sigma\to\pi\pi)} = 120$ MeV. Comparing these results with the experimental data one finds that M_σ is in satisfactory agreement with experiment, however, the decay width is very small.

5. VECTOR AND AXIAL-VECTOR MESONS

The propagators of the vector and axial-vector mesons have transversal and longitudinal parts

$$D^{\mu\nu}_{\rho,a_1} = T^{\mu\nu} D^T_{\rho,a_1} + L^{\mu\nu} D^L_{\rho,a_1}, \tag{31}$$

where $T^{\mu\nu} = g^{\mu\nu} - p^\mu p^\nu/p^2$, $L^{\mu\nu} = p^\mu p^\nu/p^2$ and

$$D^T_{\rho,a_1} = \frac{1}{G^{-1}_{\rho,a_1} + \Pi^T_{\rho,a_1}(p^2)} = \frac{g^2_{\rho,a_1}(p^2)}{M^2_{\rho,a_1} - p^2},\ D^L_{\rho,a_1} = \frac{1}{G^{-1}_{\rho,a_1} + \Pi^L_{\rho,a_1}(p^2)}. \tag{32}$$

Here, Π^T_{ρ,a_1} and Π^L_{ρ,a_1} are transversal and longitudinal parts of the polarization operator $\Pi^{\mu\nu}_{\rho,a_1}(p^2)$

$$\Pi^{\mu\nu}_{\rho,a_1}(p^2) = i\frac{2N_c}{(2\pi)^4}\int d^4k f^2(k_-) f^2(k_+)\,\mathrm{Sp}\left[\mathrm{S}(k_-)\Gamma_{\rho,a_1}\mathrm{S}(k_+)\Gamma_{\rho,a_1}\right].$$

The constants G_{ρ,a_1} are fixed by physical meson masses

$$G^{-1}_{\rho,a_1} = -\Pi^T_{\rho,a_1}(M_{\rho,a_1})$$

and numerically equal to $G_\rho = 6.44$ GeV^{-2}, $G_{a_1} = 0.739$ GeV^{-2}. Note, that there is no pole in the longitudinal part of the vector meson propagators.

The constants $g_{\rho,a_1}(M^2_{\rho,a_1})$ are equal to

$$g^{-2}_{\rho,a_1}(M^2_{\rho,a_1}) = -\frac{d\Pi^T_{\rho,a_1}(p^2)}{dp^2}\Big|_{p^2=M^2_{\rho,a_1}}. \tag{33}$$

5.1. ρ-meson and decay $\rho \to \pi\pi$

From eq.(33) we obtain $g_\rho(M_\rho) = 1.2$. The decay $\rho \to \pi\pi$ is described by the triangle diagram similar to the diagram fig.4. The amplitude for the process is

$$A^\mu_{(\rho\to\pi\pi)} = g_{(\rho\to\pi\pi)} \cdot q^\mu, \tag{34}$$

where $q = q_1 - q_2$. We obtain $g_{(\rho\to\pi\pi)} = 5.6$ and the decay width $\Gamma_{(\rho\to\pi\pi)} = 130$ MeV which is in qualitative agreement with experimental value 149.2 ± 0.7 MeV [25].

5.2. Axial-vector meson and $\pi - a_1$ mixing

For the a_1-meson constant we obtain $g_a(M_{a_1}) = 0.5$. The longitudinal component of the a_1-meson field is mixed with the pion, as it is illustrated in fig.5. The amplitude describing this mixing is

$$A^\mu_{(\pi\to a_1)}(p^2) = iC_{(\pi\to a_1)} p^\mu. \tag{35}$$

The value of the constant $C_{(\pi\to a_1)}$ is 80 MeV. The additional renormalization of the pion field is described by the ratio(see fig.6)

$$\frac{C^2_{(\pi\to a_1)}}{g^2_{a_1}(0)(G^{-1}_{a_1} + \Pi^L_{a_1}(0))} \approx C^2_{(\pi\to a_1)} G_{a_1} \approx 0.005\,. \tag{36}$$

As one can see this ratio is small and the effect of the $\pi - a_1$ mixing can be neglected.

6. DISCUSSION AND CONCLUSION

In this work we considered one of the possibilities of construction of the nonlocal chiral quark model providing absence of UV divergences and quark confinement. These features of the model are specified by the nonlocal kernel which appeared in the four-quark interaction. Such a structure of the four-quark interaction can be motivated by the instanton model [22, 24]. A similar model was considered in [17], where the nonlocal form-factor was chosen in the Gaussian form that exponentially decreases in the Euclidean domain of momenta. Recently, in [23] it was demonstrated that the functions defining the nonlocal kernel are related to the nonlocal quark condensate. From this point of view it looks more natural to require that not a form-factor, but a scalar part of the quark propagator $m(p)/(p^2 + m^2(p))$ be an entire function. Let us note that this idea is close to the method proposed in [13], where the confinement is provided by demanding the absence of poles in the quark propagator.

As it has been shown in [23], assuming that $m(p)/(p^2+m^2(p))$ is a decreasing function of p^2 in the Euclidean region leads to three different possibilities for the dynamical quark mass $m(p)$ at different values of the parameters m_q and Λ(see Sect.3). One of them has complex valued masses on the real axis and we did not consider it. The second possibility is connected with such a choice of the parameters when the function $p^2Q^2(p^2) < 1$ in the whole domain of real p^2. Then, the solution $m_-(p)$ can be used where the mass function has zero at zero quark virtuality. In this case, the main requirements of chiral models are fulfilled. However, in this version of the model the mass of the sigma meson and the strong decay widths of the σ and ρ mesons are in disagreement with experimental data.

Therefore, in the present work we studied the third possibility of the choosing of the parameters m_q, Λ when the function $p^2Q^2(p^2) = 1$ at some point $p^2 = p_0^2$. In this case $m(p)$ is the combination of the solutions $m_+(p)$, $m_-(p)$. This mass function is nonzero at $p^2 = 0$ and drops monotonically with increasing p^2. In this case, one can predict the scalar meson mass and the decay width $\rho \to \pi\pi$ which are more close to experimental values. However, the decay width $\sigma \to \pi\pi$ remains too small.

It is useful to compare some results obtained in this model with analogous results obtained in the framework of the local NJL model[6]. Let us start with the $\pi - a_1$ mixing. In the local NJL model the amplitude describing the $\pi - a_1$ mixing equals $A^{\mu(NJL)}_{(\pi\to a_1)} = i\sqrt{6}mp^\mu$, where $m = 280$ MeV is the constituent quark mass. Therefore, the coefficient $C^{(NJL)}_{(\pi\to a_1)}$ in the NJL model equals 680 MeV. This value is one order larger than in the present model. As a result it leads to the noticeable additional renormalization of the pion field in the local NJL model $\bar{g}_\pi^{(NJL)} = g_\pi^{(NJL)} \cdot Z^{1/2}$, where $Z = \left(1 - 6m^2/M^2_{a_1}\right)^{-1} \approx 1.4$, in this model $Z = 1.004$. Therefore, in the local NJL model the $\pi - a_1$ mixing play a more important role.

Let us compare also the amplitude of the decay width $\sigma \to \pi\pi$ in these models. In the local NJL model this amplitude equals $A^{(NJL)}_{\sigma\to\pi^+\pi^-} = 4mg = 2.8$ GeV (here $g = 2.5$). This amplitude is twice times larger than in the present model. However, after taking into account $\pi - a_1$ mixing this amplitude takes the form $A^{(NJL)}_{\sigma\to\pi^+\pi^-} = 4mgZ^{-1} = 2$ GeV. This leads to noticeable decrease in the decay width which becomes smaller than experimental data.

The failure of the models to describe the σ-meson is expectable. The similar problems appeared in the QCD sum rule method. In the scalar channel with vacuum quantum numbers the corrections from different sources may be valuable. Indeed, it was shown recently that the $1/N_c$ corrections in this channel are rather big[26], and thus we can not trust the results of the model in this case.

In conclusion, let us summarize the main results of this work. The pseudoscalar, scalar, vector and axial-vector sectors of the model have been considered. It was shown that the low-energy theorems are fulfilled. The masses and strong coupling constants of the mesons were calculated. The strong coupling constants of the mesons were shown to noticeably decrease with increasing p^2 in the physical domain(see fig. 2). The $\pi - a_1$ mixing was considered and it was found that this mixing could be neglected. Among satisfactory predictions of the model there are the decay width $\rho \to 2\pi$ and the mass of the sigma-meson. However, the width of decay $\sigma \to 2\pi$ is significantly below the experimental value [25].

In the future, we plan to describe the electromagnetic interactions in the framework of this model, verify the vector meson dominance, calculate the e.m. pion radius and consider the processes $\pi^0 \to \gamma\gamma$, $\gamma^* \to \gamma\pi$ (here γ^* is a virtual photon), the polarizability of the pion and the $\pi - \pi$ scattering length.

The authors thank D. Blaschke, G. V. Efimov, S. B. Gerasimov, and S. N. Nedelko for fruitful discussions. The work is supported by RFBR Grant no. 02-02-16194 and the Heisenberg–Landau program.

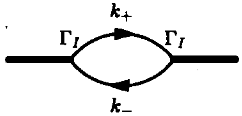

Figure 1. Meson polarization operator. The thick lines are mesons. All loops in fig.1, fig.3-fig.6 consist of constituent quarks(thin lines).

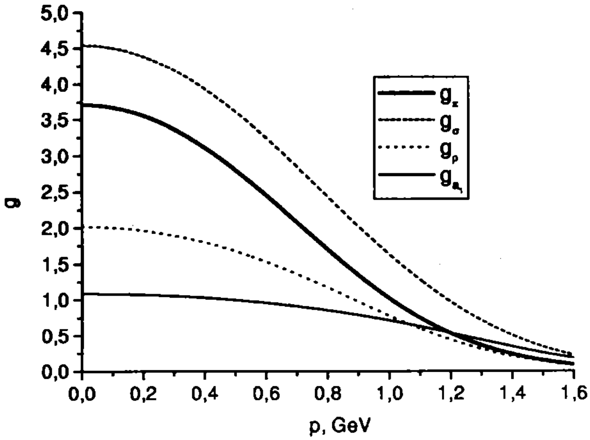

Figure 2. Momentum dependence of the mesons strong coupling constants.

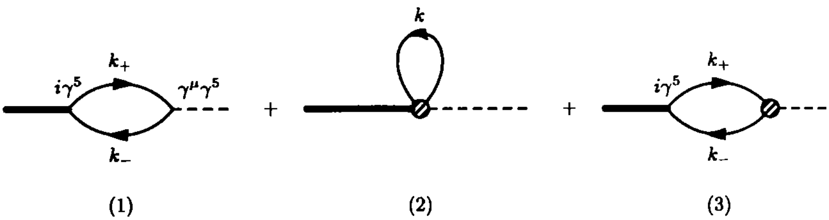

Figure 3. Weak pion decay. Dash lines denote weak external field. Blobs are nonlocal vertices.

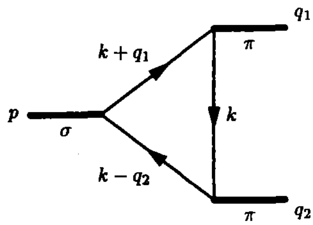

Figure 4. Decays $\sigma \to \pi\pi$, $\rho \to \pi\pi$.

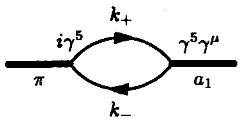

Figure 5. Transition loop describing $\pi - a_1$ mixing.

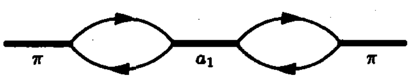

Figure 6. Diagram describing additional renormalization of the pion field.

REFERENCES

1. V. De Alfaro, S. Fubini, G. Furlan and C. Rossetti, *Currents in Hadron Physics* (American Elsevier Publishing company, New York, 1973).
2. S. Weinberg, Phys. Rev. Lett. **18**, 188 (1967);
   J. Wess and B. Zumino, Phys. Rev. **163**, 1727 (1967);
   S. Gasiorowicz and D. A. Geffen, Rev. Mod. Phys. **41**, 531 (1969).
3. Y. Nambu and G. Jona-Lasinio, Phys. Rev. **122**, 345 (1961).
4. T. Eguchi, Phys. Rev. D **14**, 2755 (1976);
   K. Kikkawa, Prog. Theor. Phys. **56**, 947 (1976).
5. M. K. Volkov and D. Ebert, Yad. Fiz. **36**, 1265 (1982);
   D. Ebert and M. K. Volkov, Z. Phys. C **16**, 205 (1983);
   M. K. Volkov, Annals Phys. **157**, 282 (1984);
   D. Ebert and H. Reinhardt, Nucl. Phys. B **271**, 188 (1986);
   D. Ebert, H. Reinhardt and M. K. Volkov, Prog. Part. Nucl. Phys. **33**, 1 (1994).
6. M. K. Volkov, Fiz. Elem. Chast. Atom. Yadra **17**, 433 (1986).
7. T. Kunihiro and T. Hatsuda, Prog. Theor. Phys. **71**, 71 (1984); Phys. Rep. **247**, 221 (1994);
   U. G. Meissner, Phys. Rep. **161**, 213 (1988);
   U. Vogl and W. Weise, Prog. Part. Nucl. Phys. **27**, 195 (1991);
   S. P. Klevansky, Rev. Mod. Phys. **64**, 649 (1992).
8. A. A. Belavin, A. M. Polyakov, A. S. Shvarts and Y. S. Tyupkin, Phys. Lett. B **59**, 85 (1975).
9. G. 't Hooft, Phys. Rev. Lett. **37**, 8 (1976).
10. C. G. Callan, R. F. Dashen and D. J. Gross, Phys. Rev. D **17**, 2717 (1978).
11. E. V. Shuryak, Nucl. Phys. B **203**, 93 (1982).
12. A. E. Dorokhov and N. I. Kochelev, Sov. J. Nucl. Phys. **52**, 135 (1990);
    A. E. Dorokhov, Y. A. Zubov and N. I. Kochelev, Sov. J. Part. Nucl. **23**, 522 (1992).
13. G. V. Efimov and M. A. Ivanov, Fiz. Elem. Chast. Atom. Yadra **20**, 1129 (1989);
    G. V. Efimov and M. A. Ivanov, *The Quark Confinement Model Of Hadrons* (IOP, Bristol, 1993) ;
    G. V. Efimov and S. N. Nedelko, Phys. Rev. D **51**, 176 (1995).

14. F. Gross, J.Milana, Phys. Rev. D **45**, 969 (1992).

15. M. Buballa and S. Krewald, Phys. Lett. B **294**, 19 (1992).

16. C. D. Roberts and A. G. Williams, Prog. Part. Nucl. Phys. **33**, 477 (1994);
C. J. Burden, L. Qian, C. D. Roberts, P. C. Tandy and M. J. Thomson, Phys. Rev. C **55**, 2649 (1997); nucl-th/9605027.

17. R. D. Bowler and M. C. Birse, Nucl. Phys. A **582**, 655 (1995); R. S. Plant and M. C. Birse, Nucl. Phys. A **628**, 607 (1998).

18. C. M. Shakin and W. D. Sun, Phys. Rev. C **54**, 1414 (1996);
L. S. Celenza, B. Huang, H. S. Wang and C. M. Shakin, Phys. Rev. C **60**, 025202 (1999).

19. K. Langfeld and M. Rho, Nucl. Phys. A **596**, 451 (1996).

20. D. Blaschke, Y. L. Kalinovsky and P. C. Tandy, in *Proceedings XI Int. Conf. on Problems of Quantum Field Theory, Dubna, Russia, 1998*, p.454; hep-ph/9811476;
D. Blaschke, G. Burau, Y. L. Kalinovsky, P. Maris and P. C. Tandy, Int. J. Mod. Phys. A **16**, 2267 (2001); nucl-th/0002024.

21. H. Ito, W. W. Buck and F. Gross, Phys. Rev. C **43**, 2483 (1991); Phys. Rev. C **45**, 1918 (1992).

22. I. V. Anikin, A. E. Dorokhov and L. Tomio, Phys. Part. Nucl. **31**, 509 (2000).

23. A. E. Dorokhov and W. Broniowski, Phys. Rev. D **65**, 094007 (2002); hep-ph/0110056.

24. D. Diakonov and V. Y. Petrov, Nucl. Phys. B **245**, 259 (1984); Nucl. Phys. B **272**, 457 (1986).

25. K. Hagiwara *et al.*, Phys. Rev. D **66**, 010001 (2002).

26. R. S. Plant and M. C. Birse, Nucl. Phys. A **703**, 717 (2002).

Received on March 17, 2003.